

Coarsening of δ -Ni₂Si precipitates in a Cu-Ni-Si alloy

メタデータ	言語: eng 出版者: 公開日: 2017-10-03 キーワード (Ja): キーワード (En): 作成者: メールアドレス: 所属:
URL	http://hdl.handle.net/2297/27791

Coarsening of δ -Ni₂Si precipitates in a Cu-Ni-Si alloy

Chihiro Watanabe* and Ryoichi Monzen

Division of Innovative Technology and Science, Kanazawa University,
Kakuma-machi, Kanazawa 920-1192, Ishikawa, Japan

*Corresponding author

E-mail: chihiro@t.kanazawa-u.ac.jp, TEL: +81-76-234-4677, Fax: +81-76-234-6424

Abstract

The coarsening behavior of rod-shaped and spherical δ -Ni₂Si precipitates in a Cu-1.86wt%Ni-0.45wt%Si alloy during aging at 823 to 948 K has been investigated by measuring both precipitate size by transmission electron microscopy (TEM) and solute concentration in the Cu matrix by electrical resistivity. The rod-shaped δ precipitates have an elongated shape along $\langle 558 \rangle_m$ and a $\{110\}_m$ habit-plane facet. The coarsening theory of a spherical precipitate in a ternary alloy developed by Kuehmann and Voorhees (KV) has been modified to a case of rod-shaped precipitates. The coarsening kinetics of average size of the rod-shaped and spherical δ precipitates with aging time t obey the $t^{1/3}$ time law, as predicted by the modified KV theory. The kinetics of depletion of the supersaturation with t are coincident with the predicted $t^{-1/3}$ time law. Application of the modified KV theory has enabled calculation of the energies of sphere, $\{110\}_m$ and rod-end interfaces from the data on coarsening alone. The energy of the $\{110\}_m$ interface having a high degree of coherency to the Cu matrix is estimated to be 0.4 Jm^{-2} , the incoherent sphere-interface energy 0.6 Jm^{-2} , and the rod-end interface energy 5.2 Jm^{-2} .

Keywords: Coarsening theory, Interface energy, Ni₂Si precipitate, Copper-nickel-silicon alloy

Introduction

Kuehmann and Voorhees (KV) [1] have developed a theory for the coarsening of a spherical precipitated phase having two chemical components in a ternary alloy. By formulating the Gibbs-Thompson equation for the ternary system, they found that the temporal power law of the average particle radius, far-field-matrix supersaturation and particle number density were identical to those of the coarsening theory of Lifshitz and Slyozov [2] and Wagner [3] (LSW) but the amplitudes of these power laws were different from the LSW theory. The theories of LSW, LSW modified by Ardell [4], and KV have already been employed to study the Ostwald ripening processes of spherical second-phase precipitates in actual alloys [5-9]. However, the actual shapes of second-phase particles are usually non-spherical.

In a previous paper [10], Watanabe et al. have extended the KV theory to a general case of second-phase particles with any centro-symmetric shape. They applied the generalized KV theory to the experimental data on the coarsening of spherical, {001}-faceted cuboidal and {111}-faceted octahedral Co, Fe and Co-Fe precipitates with a face-centered cubic structure in a Cu-Co alloy, a Cu-Fe alloy and three Cu-Co-Fe alloys with different Co and Fe contents during ageing at 873 to 973 K, and then estimated the energies for sphere, {001} and {111} interfaces. Recently, we have examined the Ostwald ripening of {001}-faceted cuboidal Al₃Sc precipitates in an Al-1wt%Mg-0.27wt%Sc alloy aged at 698, 723 and 748 K from measurements of the precipitates size by transmission electron microscopy (TEM) and the solute concentration in the Al matrix by electrical resistivity [11]. By applying the generalized KV theory to the coarsening data, the {001} interface energy were obtained without assuming values of the diffusivity of solute atoms in the matrix. The estimated value of interface energy is in excellent agreement with that obtained using the first-principles calculation method [12].

Aging of solutionized Cu-Ni-Si alloys first produces disk-shaped δ -Ni₂Si precipitates [13, 14]. The δ precipitates have a facet of habit plane parallel to the matrix {110}_m plane [13]. On further aging, the disk-shaped δ precipitates rapidly grow into a rod shape elongated parallel to the invariant line direction of $\langle 558 \rangle_m$ [15]. We have found that, after recrystallization on annealing of an aged and deformed Cu-Ni-Si alloy, δ precipitates exhibit no specific orientation relationship to the Cu matrix of recrystallized grains and, as a result, the shape of the δ precipitates remains nearly spherical even after prolonged aging.

In this study, the coarsening behavior of both the rod-shaped and spherical δ precipitates in a Cu-1.86wt%Ni-0.45wt%Si alloy is investigated by measuring both the precipitate size by TEM and the solute concentration in the Cu matrix by electrical resistivity. The KV theory of a spherical precipitate in a ternary alloy is modified to a case of rod-shaped precipitates. The interface energies between the Cu matrix and the spherical and rod-shaped precipitates are estimated using the modified KV theory.

Modification of KV theory to rod-shaped precipitate

First, we will extend the KV theory of a spherical precipitate to a rod-shaped precipitate. Let us consider a ternary system, consisting of solvent (1) and two solutes (2) and (3). A rod shape is approximated by

a prolate spheroid with $l \gg w$, where l is the length of the rod and w is length of radial axis of the rod. Ham has shown that the flux to such rod-shaped precipitates is given by [16]

$$\dot{Q}_i = -\frac{2\pi w D_i A}{\hat{C}_i^\beta V_m \ln(2A)} (\hat{C}_i^\alpha - \bar{C}_i^\alpha) \quad (i = 2, 3) \quad (1)$$

where \dot{Q}_i is the flux of the i th component, D_i is the diffusion coefficient, V_m is the molar volume of a β phase precipitate, A is the aspect ratio of l/w , $\hat{C}_i^{\alpha/\beta}$ is the concentration of the i th component in the matrix of α phase or the β precipitate at the α/β interface, and $\bar{C}_i^{\alpha/\beta}$ is the concentration far from the α/β interface. Eq.

(1) necessitates that the precipitate shape is unchanged. From the mass conservation, the flux \dot{Q}_i must be equal to volume change of the precipitated phase. Thus we have

$$\dot{Q}_i = -\frac{\hat{C}_i^\beta - \hat{C}_i^\alpha}{\hat{C}_i^\beta V_m} \frac{dV}{dt} \quad (2)$$

where V is the volume of the β precipitate and is expressed as

$$V = \frac{2}{3}\pi \left(\frac{w}{2}\right)^2 l = \frac{4}{3}\pi \left(\frac{w}{2}\right)^3 A \quad (3)$$

Eqs. (1) to (3) yield the growth rate $\dot{w} = dw/dt$ of the rod-shaped precipitate as

$$\dot{w} = -\frac{4D_i}{w \ln(2A)} \frac{\hat{C}_i^\alpha - \bar{C}_i^\alpha}{\hat{C}_i^\beta - \hat{C}_i^\alpha} \quad (4)$$

Following Kuehmann and Voorhees [1], we have a good approximation during coarsening that

$$\frac{\hat{C}_2^\alpha - \bar{C}_2^\alpha}{\hat{C}_3^\alpha - \bar{C}_3^\alpha} \frac{D_2}{D_3} = \frac{\Delta C_2}{\Delta C_3} \quad (5)$$

where $\Delta C_i = \hat{C}_i^\beta - \hat{C}_i^\alpha \approx C_i^\beta - C_i^\alpha$ and C_i^α and C_i^β are the equilibrium solubilities of the component i in the α and β phases.

Johnson generalized the Gibbs-Thompson equation to any precipitate with three-dimensionally-point symmetric shape [17]. According to Johnson, the Gibbs-Thompson equation for the rod-shaped precipitates is expressed as

$$\mu_m(w) - \mu_m(\infty) = \frac{4\gamma_w}{w} V_m = \frac{4\gamma_l}{l} V_m \quad (6)$$

where $\mu_m(w)$ is the chemical potential of the matrix in equilibrium with the rod-shaped β precipitate with radial length w , $\mu_m(\infty)$ is that of the matrix in equilibrium with a flat surface of the same substance, and γ_w and γ_l are energies of lateral and end cusp interfaces of the rod, respectively. The Gibbs-Thompson equation for a ternary system has already obtained by Kuehmann and Voorhees [1]. From their results with Eq. (6), the Gibbs-Thompson equations for the rod-shaped precipitate are expressed as

$$\hat{C}_2^\alpha - C_2^\alpha = \frac{\Delta C_2}{D_2} \frac{4\gamma_w V_m}{\Lambda} \frac{1}{w} + \frac{\Delta C_2 G_{23}^\alpha + \Delta C_3 G_{33}^\alpha}{\Lambda} \left[\frac{\Delta C_3}{D_3} (\bar{C}_2^\alpha - C_2^\alpha) - \frac{\Delta C_2}{D_2} (\bar{C}_3^\alpha - C_3^\alpha) \right] \quad (7)$$

$$\hat{C}_3^\alpha - C_3^\alpha = \frac{\Delta C_3}{D_3} \frac{4\gamma_w V_m}{\Lambda} \frac{1}{w} + \frac{\Delta C_2 G_{22}^\alpha + \Delta C_3 G_{23}^\alpha}{\Lambda} \left[\frac{\Delta C_2}{D_2} (\bar{C}_3^\alpha - C_3^\alpha) - \frac{\Delta C_3}{D_3} (\bar{C}_2^\alpha - C_2^\alpha) \right] \quad (8)$$

here
$$\Lambda = \frac{\Delta C_2}{D_2} (\Delta C_2 G_{22}^\alpha + \Delta C_3 G_{23}^\alpha) + \frac{\Delta C_3}{D_3} (\Delta C_2 G_{23}^\alpha + \Delta C_3 G_{33}^\alpha), \quad (9)$$

$$G_{ij}^\alpha = \frac{\partial G^\alpha}{\partial C_i^\alpha \partial C_j^\alpha} \quad (i \text{ or } j = 2 \text{ and } 3) \quad (10)$$

and G^α is the Gibbs free energy of the α phase. Using Eqs. (4), (7) and (8), the precipitate growth rate \dot{w} is related to the size w and the supersaturations at infinity as

$$\dot{w} = \frac{4}{\Lambda w \ln(2A)} \left[(\Delta C_2 G_{22}^\alpha + \Delta C_3 G_{23}^\alpha) (\bar{C}_2^\alpha - C_2^\alpha) + (\Delta C_2 G_{22}^\alpha + \Delta C_3 G_{23}^\alpha) (\bar{C}_3^\alpha - C_3^\alpha) - \frac{4\gamma_w V_m}{w} \right] \quad (11)$$

The mathematical treatments to obtain asymptotic solutions of Eq. (11) have been already reported by Marqusee and Ross [18] and Voorhees [19]. Thus we will only state the results of this analysis. The cube of the average size of rods \bar{w}^3 is given by

$$\bar{w}^3 - \bar{w}_0^3 = K_w t \quad (12)$$

$$K_w = \frac{64\gamma_w V_m}{9\Lambda \ln(2A)} \quad (13)$$

where K_w is the coarsening rate constant. The far-field supersaturation for the component i is

$$\bar{C}_i^\alpha - C_i^\alpha = k_i t^{-1/3} \quad (14)$$

$$k_i = \frac{(3\gamma_w V_m)^{2/3} [\Lambda \ln(2A)]^{1/3} \Delta C_i}{(\Delta C_2 G_{22}^\alpha + \Delta C_3 G_{23}^\alpha) \Delta C_2 + (\Delta C_2 G_{22}^\alpha + \Delta C_3 G_{23}^\alpha) \Delta C_3} \quad (15)$$

here k_i is the coarsening parameter. Finally, we summarize the assumption for application of the KV theory modified to the rod-shaped precipitate: (i) the precipitate shape remains unchanged during coarsening and (ii) the system is a dilute solution.

Experimental procedure

Cu alloy ingot containing 1.86wt%Ni and 0.45wt%Si were prepared in a melting furnace under an Argon atmosphere. The ingot was homogenized at 1273K for 24h in the argon atmosphere. Specimens cut from the alloy ingot were cold-rolled to the reduction of 50% in thickness, solution treated at 1273K for 3h and subsequently quenched into cold water. One set of the solutionized specimens were aged at 923 and 948K to obtain rod-shaped δ -Ni₂Si precipitates. Second set of the specimens were aged at 748K for 14h and rolled to 85% reduction. The cold-rolled specimen sheets were then annealed at 873K for 10min. The annealing caused complete recrystallization of the specimens. The annealed specimens had nearly spherical δ precipitates with an average radius of 25nm. Aging was again carried out at 823, 873, 923 and 948K.

Three millimeter diameter disks were punched from the aged specimens, mechanically ground down to 0.2mm, and electro-polished using a solution 20% phosphoric acid at 273K. Microscopy was performed using a JEOL 2000EX and a 2010FEF microscope at an operation voltage of 200kV. The average size of precipitates

was measured from bright-field TEM images of the precipitates. To obtain statistically reliable data, more than 200 precipitates were analyzed for each aging condition.

The specimens for electrical resistivity measurements were cut to a size of 70 x 15 x 0.3 mm³. After aging, resistivity measurements were made at room temperature (293K) using a standard four-point potentiometric technique. The measurements were repeated ten times to obtain one data point, reversing the current direction to eliminate the stray electromotive force.

Results and discussion

Microstructure

Similar to the previous studies [13, 14], small disk-shaped δ -Ni₂Si first appeared in the Cu matrix by aging of the supersaturated Cu-Ni-Si alloy at 923 and 948 K. The disk-shaped δ precipitates has a faceted habit plane parallel to the matrix $\{110\}_m$ [13]. Prolonged aging caused the preferential growth of the δ precipitates along certain crystallographic directions, which are parallel to the invariant line directions of $\langle 558 \rangle_m$ [15]. Figure 1(a) depicts rod-shaped δ precipitates in the alloy aged at 923 K for 42 h. Figure 1(b) shows the cross-sectional view of a rod-shaped δ precipitate. The elongated $[85\bar{5}]_m$ direction is perpendicular to the micrograph. As can be seen in Fig. 1(b), the rod-shaped δ precipitate maintains the identical habit plane parallel to the $(011)_m$. The $\{110\}_m$ habit planes were universally observed in all the precipitates examined. From analyses of selected-area diffraction patterns (SADPs) taken from several regions containing rod-shaped δ precipitates, an orientation relationship was found between the Cu matrix and the δ precipitate:

$$[100]_m // [001]_p; (011)_m // (010)_p.$$

This orientation relationship is in agreement with that previously reported in the literature [13, 14]. On the other hand, the δ precipitates in a deformed and recrystallized alloy exhibited no specific orientation relationship to the Cu matrix of grains. As a result, the shape of the δ precipitates was nearly spherical consistently during aging at 823, 873, 923 and 948 K, as exemplified in Fig. 2.

Coarsening kinetics of rod-shaped δ precipitates

For the rod-shaped δ precipitate, the length l along the elongated direction ($\langle 558 \rangle_m$), the width w_1 along the habit plane normal ($\langle 110 \rangle_m$) and the width w_2 perpendicular to both the elongated direction and habit plane normal were measured as the sizes of precipitates. Figure 3 displays the average precipitate sizes \bar{w}_1 , \bar{w}_2 and \bar{l} against aging time t on logarithmic scales. According to Eqs. (12) and (13), the slopes of Figs. 3 yield a time exponent. Excepting at early times, the experimental slopes are almost identical to the value of 1/3, predicted by the modified KV theory. Deviation of the slopes from 1/3 in the initial stage of aging could be an indication that the system is in a transient regime before reaching a coarsening stage. Figure 4 shows the values of \bar{w}_2/\bar{w}_1 and the aspect ratio A of \bar{l}/\bar{w}_1 against t . The value of \bar{w}_2/\bar{w}_1 was almost constant from an early stage of aging and was about 2. However, the aspect ratio A rapidly increased with aging time and reached the

saturated value of about 13 above about 42 h (1.51×10^5 s) and 18 h (6.48×10^4 s) at 923 and 948K, respectively. These times are identical to those above which, in Fig. 6, the kinetics of the decay of supersaturation with t on aging at the temperatures obey the prediction of the modified KV theory. Therefore, the coarsening of the rod-shaped precipitates begins over about 1.51×10^5 s at 923K and 6.48×10^4 s at 948K.

Data on coarsening for the rod-shaped precipitates were then obtained after the value of A was saturated to 13. Figure 5 depicts the coarsening curves of the rod-shaped δ precipitates in the present alloy aged at 923 and 948K. A linear relationship exists between \bar{w}_1 and t . Experimental values of coarsening rate constant K_w were determined from the slopes of the straight lines in Fig. 5, and Table 1 lists the values of K_w .

The solute concentration \bar{C}_i^α in the Cu matrix were obtained by the electrical resistivity method with the relations of $\Delta\rho_{Ni}=1.1 \times 10^{-8} \Omega \text{ m/at\%}$ and $\Delta\rho_{Si}=3.1 \times 10^{-8} \Omega \text{ m/at\%}$ [20], taking the atomic ratio of Ni/Si=2 into account. Here, $\Delta\rho_{Ni}$ and $\Delta\rho_{Si}$ are the ratio of resistivity increments by solute Ni and Si atoms. Following Eqs. (14) and (15), \bar{C}_i^α versus $t^{1/3}$ was plotted for the alloys aged at 923 and 948K, as shown in Fig. 6. For both aging temperatures, it is seen that \bar{C}_i^α rapidly decreases at the initial stage of aging and, over a time, a linearity exist between \bar{C}_i^α and $t^{1/3}$. The rapid decrease in \bar{C}_i^α should correspond to nucleation and growth stages of the precipitates. The slopes of these lines give experimental values of $k_i^{-1/3}$. Table 2 lists the values of $k_i^{-1/3}$, determined by the least-squares fits. Also extrapolation to $t^{1/3}=0$ ($t \rightarrow \infty$) yields values of equilibrium solubility C_i^α . Table 3 summarizes these values.

Coarsening kinetics of spherical δ precipitates

The KV theory of coarsening for spherical precipitates in ternary system predicts that the cube of average radius \bar{r}^3 increase with time t , as follows [1]:

$$\bar{r}^3 - \bar{r}_0^3 = K_s t \quad (16)$$

$$K_s = \frac{8\gamma_s V_m}{9\Lambda} \quad (17)$$

where K_s is the coarsening rate constant for the spherical δ precipitate and γ_s is isotropic interface energy between the Cu matrix and δ -Ni₂Si precipitate. Coarsening curves of the spherical δ precipitates in the present alloy aged at 823, 873, 923 and 948K are presented in Fig. 7. The slopes of the straight lines, determined by the least-squares method, give experimental values of K_s . The obtained values of K_s are listed in Table 1.

As shown in our previous paper [10], the size distributions of 3-dimensionally-point symmetric particles in ternary systems follow the distribution function of the LSW theory. A comparison between the measured and the theoretically predicted size distributions were then conducted. For the rod-shaped precipitates, the radius of a sphere with volume identical to that of the rod was used as a size of the precipitates. In the early stage of aging at each temperature, the experimental histograms for the rod-shaped and spherical precipitates were in good agreement with the LSW distribution, but this agreement does not last as a function of aging time. The size distributions generally became broader with time. The broader shapes of histograms of larger

precipitates are similar to those predicted by the theories of Ardell [21], Voorhees and Glicksman [22] and Wang et al. [23], considering the effect of precipitate volume fraction on coarsening.

According to the KV theory, the depletion of solute concentration \bar{C}_i^α in the matrix during coarsening of spherical precipitates obeys $t^{-1/3}$ time law, as shown in Eq. (14) [1]. However, the coarsening parameter k_i is a different form, and expressed as [1]

$$k_i = \frac{(3\gamma_s V_m)^{2/3} \Lambda^{1/3} \Delta C_i}{(\Delta C_2 G_{22}^\alpha + \Delta C_3 G_{23}^\alpha) \Delta C_2 + (\Delta C_2 G_{22}^\alpha + \Delta C_3 G_{23}^\alpha) \Delta C_3} \quad (18)$$

Following Eq. (14), plots of \bar{C}_i^α versus $t^{-1/3}$ for the alloy aged at 923 and 948K are shown in Fig. 8. In contrast to the rod-shaped precipitates (Fig. 6), a liner relationship holds between \bar{C}_i^α and $t^{-1/3}$ from the early stage of aging. As described in above, to obtain spherical precipitates, a portion of specimens were annealed at 873K after aging at 748K and subsequent cold-rolling. During the annealing at 873K, supersaturated solute atoms in the matrix tend to be captured by the existing precipitates. This qualitatively explains the absence in nucleation and growth stages in Figs. 7 and 8. The slopes and intercepts of the straight lines yield values of $k_i^{-1/3}$ and C_i^α , which are summarized in Table 2 and 3, respectively. Although, the reliable solvus curve for the Cu- δ -Ni₂Si quasi binary system has not yet been reported, we feel that the reliability of these values is high since the values of C_i^α for 923 and 948K obtained for the alloys bearing rod-shaped and spherical δ precipitates are almost the same.

Calculation of interface energy from experimental data

Using the subregular solution model, we have following expressions:

$$G_{\text{NiNi}}^\alpha = \frac{RT(1 - \bar{C}_{\text{Si}}^\alpha)}{\bar{C}_{\text{Ni}}^\alpha(1 - \bar{C}_{\text{Ni}}^\alpha - \bar{C}_{\text{Si}}^\alpha)} - 2L_{\text{CuNi}} - 2L_{\text{CuNiSi}}\bar{C}_{\text{Si}}^\alpha \quad (19)$$

$$G_{\text{NiSi}}^\alpha = \frac{RT}{1 - \bar{C}_{\text{Ni}}^\alpha - \bar{C}_{\text{Si}}^\alpha} - L_{\text{CuNi}} - L_{\text{CuSi}} - L_{\text{NiSi}} - L_{\text{CuNiSi}}(1 - \bar{C}_{\text{Ni}}^\alpha - \bar{C}_{\text{Si}}^\alpha) \quad (20)$$

$$G_{\text{SiSi}}^\alpha = \frac{RT(1 - \bar{C}_{\text{Ni}}^\alpha)}{\bar{C}_{\text{Si}}^\alpha(1 - \bar{C}_{\text{Ni}}^\alpha - \bar{C}_{\text{Si}}^\alpha)} - 2L_{\text{CuSi}} - 2L_{\text{CuNiSi}}\bar{C}_{\text{Ni}}^\alpha \quad (21)$$

where RT has its usual meaning, L_{ij} is the interaction parameter between i and j atoms (i or j = Cu, Ni and Si) and L_{CuNiSi} is the ternary interaction parameter. The values of L_{CuNi} , L_{CuSi} , L_{NiSi} and L_{CuNiSi} were calculated from the literature [24]. For the later stage of aging where the coarsening of the precipitates only is taking place, $\bar{C}_{\text{Ni}}^\alpha$ and $\bar{C}_{\text{Si}}^\alpha$ can be approximated to C_{Ni}^α and C_{Si}^α , respectively. The solute concentration in the Cu matrix is negligibly small compared to that in the precipitate phase at any time (Figs. 6 and 8), and thus we obtain $\Delta C_{\text{Ni}} \approx 0.67$ and $\Delta C_{\text{Si}} \approx 0.33$.

Combination of the K_w or K_s and k_i enables the matrix / precipitate interface energy γ_w or γ_s to be calculated without having to assume the values of D_{Ni} and D_{Si} :

$$\gamma_j = \frac{K_j^{1/3} k_i}{2V_m \Delta C_i} \left[\Delta C_{Ni} \left(\Delta C_{Ni} G_{NiNi}^\alpha + \Delta C_{Si} G_{NiSi}^\alpha \right) + \Delta C_{Si} \left(\Delta C_{Ni} G_{NiSi}^\alpha + \Delta C_{Si} G_{SiSi}^\alpha \right) \right] \quad (j = w \text{ or } s). \quad (22)$$

The value of V_m was calculated as $6.59 \times 10^{-6} \text{m}^3 \text{mol}^{-1}$ from $V_m = N_a abc / 12$, where N_a is the Abogadro number and a , b and c is the lattice constants of δ -Ni₂Si phase [25]. The energies γ_s and γ_w for sphere and $\{110\}_m$ interfaces obtained from Eq. (22) are listed in Table 4. From Eq. (6) with the saturated value of A ($=13$), the rod-end interface energy γ_l of the rod-shaped δ precipitate was also estimated using the value of γ_w , as shown in Table 4. Onaka et al. [26] have theoretically and experimentally shown shape of the precipitates in a matrix is determined so as to minimize the sum of the elastic strain and interface energies of the precipitates, indicating that the Wulff construction is not valid in actual alloy systems. One would then consider that the elastic strain energy results in errant estimates of the interface energies. In a literature [10], the coarsening kinetic of second-phase precipitates at a given temperature is dependent upon the interface energy alone. Therefore, we believe that the KV theory modified in present study can estimate the proper interface energy.

The experimentally obtained value of γ_s is similar to the isotropic interface energy of 0.5Jm^{-2} for incoherent spherical α -Fe precipitates in the Cu matrix, obtained using the LSW theory by TEM and electrical resistivity [27]. The value of $\gamma_s = 0.6 \text{Jm}^{-2}$ can thus be reasonably accepted as the incoherent Cu/ δ -Ni₂Si interface energy. On the other hand, the energy of the rod-end interface is much larger than that of sphere interface. In this study, a rod shape is approximated by a prolate spheroid. This approximation overestimates a curvature of the rod-end and would consequently lead to an overestimate of the energy of rod-end interface.

According to the orientation relationship between the Cu matrix and δ precipitates mentioned above, the $(0\bar{1}1)_m$ plane lying normal to the $(011)_m$ habit plane is parallel to $(100)_p$, and the $(100)_m$ plane is parallel to the $(001)_p$ plane. The misfit strain $\delta_{0\bar{1}1_m}$ along the $[0\bar{1}1]_m$ on the habit plane is expressed as $(d_{0\bar{1}1_m} - d_{100_p}) / d_{0\bar{1}1_m}$, where $d_{0\bar{1}1_m}$ and d_{100_p} are the spacings of $(0\bar{1}1)_m$ and $(100)_p$, respectively. Using the lattice parameters of the Cu matrix and δ -Ni₂Si phase, $\delta_{0\bar{1}1_m}$ is calculated as 2.3%. In the same manner, the misfit strain along the $[100]_m$ direction is estimated as $\delta_{100_m} \approx -2.9\%$. The relatively small misfit strains along $[0\bar{1}1]_m$ and $[100]_m$ directions, lying in the habit plane, suggest that there is possible lattice continuity between the matrix and precipitate across the habit plane. Lockyer and Noble [13] reported, from analyses of SADPs, that the δ precipitates in the Cu matrix is elastically distorted and, as a result, misfit strains between the matrix and precipitate are relaxed into about half values. Therefore, it is said that the interface between the precipitate and habit plane hold a high degree of coherency. The result shown in Table 4 that the interface energy of highly coherent $\{110\}_m$ habit plane is the lowest of the three energies can thus be reasonably understood.

Calculation of diffusion coefficient from experimental data

By combining Eqs (13) and (15) and Eqs. (17) and (18), the diffusion coefficient D_{Ni} of Ni in the Cu was deduced with the relation of D_{Ni} [28] $\ll D_{Si}$ [24] that

$$D_{\text{Ni}} = \frac{9K_w^{2/3} \Delta C_{\text{Ni}} \ln(2A)}{4k_{\text{Ni}} \left[\Delta C_{\text{Ni}} (\Delta C_{\text{Ni}} G_{\text{NiNi}}^\alpha + \Delta C_{\text{Si}} G_{\text{NiSi}}^\alpha) + \Delta C_{\text{Si}} (\Delta C_{\text{Ni}} G_{\text{NiSi}}^\alpha + \Delta C_{\text{Si}} G_{\text{SiSi}}^\alpha) \right]} \quad \text{for the rod} \quad (23)$$

and

$$D_{\text{Ni}} = \frac{9K_s^{2/3} \Delta C_{\text{Ni}}}{4k_{\text{Ni}} \left[\Delta C_{\text{Ni}} (\Delta C_{\text{Ni}} G_{\text{NiNi}}^\alpha + \Delta C_{\text{Si}} G_{\text{NiSi}}^\alpha) + \Delta C_{\text{Si}} (\Delta C_{\text{Ni}} G_{\text{NiSi}}^\alpha + \Delta C_{\text{Si}} G_{\text{SiSi}}^\alpha) \right]} \quad \text{for sphere.} \quad (24)$$

Using experimental values of K_w or K_s and k_i , C_{Ni}^α and C_{Si}^α , values of D_{Ni} were calculated by Eqs. (23) and (24). Figure 9 presents the Arrhenius plots of D_{Ni} as a function of T^{-1} , together with the impurity diffusion data obtained using a tracer diffusion technique by Almazouzi *et al.* From the intercept and slope of the straight line fitted to the D_{Ni} data for the spherical precipitates, the pre-exponential factor D_0 and the activation energy Q were calculated. The estimated values of D_0 and Q are $(2.7 \pm 1.0) \times 10^{-4} \text{m}^2 \text{s}^{-1}$ and $222 \pm 3 \text{kJ/mol}^{-1}$, which agrees reasonably with the values of $0.62 \times 10^{-4} \text{m}^2 \text{s}^{-1}$ and 224kJ/mol^{-1} for the impurity diffusion of Ni in Cu.

Conclusions

- (1) The theory of Ostwald ripening of spherical precipitates in ternary systems developed by Kuehmann and Voorhees (KV) [1] has been modified to rod-shaped precipitates. The time exponents of the average precipitate size and supersaturation at infinity are identical to those found by KV.
- (2) The Ostwald ripening of rod-shaped and spherical δ -Ni₂Si precipitates in a Cu-1.86wt%Ni-0.45wt%Si alloy during aging at 823 to 948 K has been examined by the combined technique of transmission electron microscopy observations and electrical resistivity measurements. The rod-shaped δ precipitates have an elongated shape along $\langle 558 \rangle_m$, (which is parallel to the invariant line direction [15],) and have a $\{110\}_m$ habit plane, across which there is a high degree of coherency. The average sizes of the rod-shaped and spherical δ precipitates increase with aging time t as $t^{1/3}$, as predicted by the KV and modified KV models. The kinetics of the decay of the matrix supersaturation follow the predicted $t^{-1/3}$ law.
- (3) By applying the KV and modified KV models to the coarsening data of spherical and rod-shaped δ precipitates in the Cu matrix, the energy γ of sphere, $\{110\}_m$ or rod-end interface and the diffusivity D of Ni in Cu have been independently derived. The values of γ for the $\{110\}_m$ habit plane with a high degree of coherency to the Cu matrix, the incoherent sphere-interface and rod-end interface are found to be 0.4Jm^{-2} , 0.6Jm^{-2} and 5.2Jm^{-2} , respectively. The estimate of D is nearly identical to reported impurity diffusion data for Ni in Cu [28].

Figure & table captions

Fig. 1 (a) Bright field image of rod-shaped δ -Ni₂Si precipitates and in a Cu-Ni-Si specimen aged at 923 K for 42 h. The zone axis is [011]_m. (b) Cross-sectional view of a rod-shaped δ -Ni₂Si precipitate in the same specimen. The zone axis is [855]_m parallel to the growth direction of the precipitate.

Fig. 2 Bright field image of nearly spherical δ -Ni₂Si precipitates in a Cu-Ni-Si alloy aged at 923 K for 42 h after recrystallization of the alloy. The zone axis is [011]_m.

Fig. 3 Change in the average sizes \bar{w}_1 , \bar{w}_2 , and \bar{l} of rod-shaped δ -Ni₂Si precipitates with aging time for a Cu-Ni-Si alloy aged at (a) 923 and (b) 948 K.

Fig. 4 Change in the aspect ratios \bar{l}/\bar{w}_1 , \bar{w}_2/\bar{w}_1 during aging of a Cu-Ni-Si alloy at 923 and 948 K.

Fig. 5 Coarsening curves for rod-shaped δ -Ni₂Si precipitates in a Cu-Ni-Si alloy aged at 923 and 948 K.

Fig. 6 Change in the solute concentration \bar{C}_i^α in the matrix of a Cu-Ni-Si alloy bearing rod-shaped δ -Ni₂Si precipitates during aging at 923 and 924 K.

Fig. 7 Coarsening curves for spherical δ -Ni₂Si precipitates in a Cu-Ni-Si alloy aged at 823, 873, 923 and 948 K after recrystallization of the alloy.

Fig. 8 Change in the solute concentration \bar{C}_i^α in the matrix of a Cu-Ni-Si alloy bearing spherical δ -Ni₂Si precipitates during aging at 923 and 924 K after recrystallization of the alloy.

Fig. 9 Comparison of the diffusivity values of Ni in Cu obtained in the present study with those available in the literature by Almazouzi *et al* [28].

Table 1 Values of the coarsening rate constants K_w and K_s for rod-shaped and spherical δ -Ni₂Si precipitates.

Table 2 Values of the coarsening parameter k_i for rod-shaped and spherical δ -Ni₂Si precipitates.

Table 3 Values of the equilibrium solubility of Ni and Si in the Cu matrix bearing rod-shaped and spherical δ -Ni₂Si precipitates.

Table 4 Energies γ of {110}_m, rod-end and sphere interfaces of δ -Ni₂Si precipitates in a Cu-Ni-Si alloy, estimated using Eq. (19).

References

- [1] Kuehmann CJ, Voorhees PW (1996) *Metall Mater Trans A* 27:937-943.
- [2] Lifshitz IM, Slyozov VV (1961) *J Phys Chem Solids* 19:35-50.
- [3] Wagner C (1961) *Z Elektrochem* 65:581-591.
- [4] Ardell AJ (1967) *Acta Metall* 15:1772-75.
- [5] Chellman DJ, Ardell AJ (1974) *Acta Metall* 22:577-88.
- [6] Noble B, Bray SE (1999) *Phil. Mag A* 79:859-872.
- [7] Marquis EA, Seidman DN (2005) *Acta Mater* 53:4259-4268
- [8] Watanabe C, Watanabe D, Monzen R (2006) *Mater Trans* 47:2285-2291
- [9] Watanabe C, Watanabe D, Monzen R (2008) *J Mater Sci* 43:3817-3824.
- [10] Watanabe D, Watanabe C, Monzen R (2009) *Acta Mater* 57:1899-1911.
- [11] Watanabe C, Watanabe D, Tanii R, Monzen R (2010) *Phil Mag Lett* 90:103-111.
- [12] Asta M, Foiles MS, Quong AA (1998) *Phys Rev B* 57:11265-11275.
- [13] Locker SA, Noble FW (1994) *J Mater Sci* 29:218-226.
- [14] Fujiwara H, Sato T, Kamio A (1998) *J Japan Inst Metals* 62:301-309.
- [15] Ono R, Kanmuri K, Fukamachi K, Fujii T, Onaka S, Kato M (2004) *J JRICu* 43:45-46.
- [16] Ham FS (1958) *J Phys Chem Solids* 6:335-351.
- [17] Johnson CA (1965) *Sur Sci* 3:429-444.
- [18] Marqusee JA, Ross J (1983) *J Chem Phys* 79:373-378.
- [19] Voorhees PW (1990) *Metall Trans A* 21:27-37.
- [20] Pawlek F, Reichel K (1956) *Z Metallk* 47:347-356.
- [21] Ardell AJ (1972) *Acta Metall* 20:61-71.
- [22] Voorhees PW, Glicksman ME (1984) *Metall Trans A* 15:1081-1088.
- [23] Wang KG, Glicksman ME, Rajan K (2005) *Comput Mater Sci* 34:235-253.
- [24] Miettinen J (2005) *CALPHAD* 29:212-221.
- [25] Toman K (1952) *Acta Cryst* 5:329-331.
- [26] Onaka S, Kobayashi N, Fujii T, Kato M (2003) *Mater Sci Eng A* 347:42-49.
- [27] Monzen R, Kita K (2002) *Phil. Mag. Lett.* 82:373-382.
- [28] Almazouzi A, Macht MP, Naundorf V, Neumann G (1996) *Phys Rev B* 54:857-863.

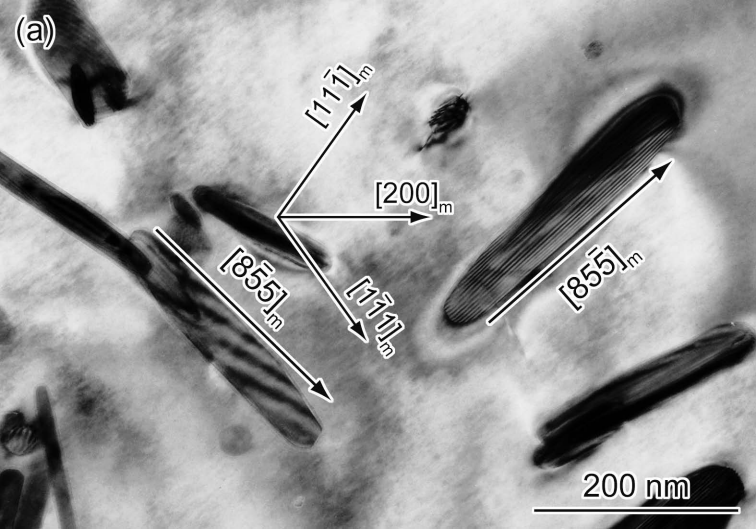
T [K]	K [m ³ s ⁻¹]	
	rod	sphere
823	-	1.34×10^{-29}
873	-	1.23×10^{-28}
923	1.69×10^{-28}	9.92×10^{-28}
948	3.76×10^{-28}	2.32×10^{-27}

T [K]	$k_{\text{Ni}} / 10^{-2} [\text{s}^{1/3}]$		$k_{\text{Si}} / 10^{-2} [\text{s}^{1/3}]$	
	rod	sphere	rod	sphere
823	-	2.83	-	1.42
873	-	1.97	-	0.98
923	3.24	1.51	1.62	0.75
948	2.85	1.26	1.42	0.63

T [K]	C_{Ni^α} [at%]		C_{Si^α} [at%]	
	rod	sphere	rod	sphere
823	-	0.46	-	0.23
873	-	0.67	-	0.34
923	0.94	0.95	0.47	0.47
948	1.06	1.07	0.53	0.53

T [K]	γ [Jm ⁻²]		
	$\{110\}_m$	rod-end	sphere
823	-	-	0.62
873	-	-	0.62
923	0.42	5.46	0.64
948	0.40	5.20	0.63

(a)



(b)

$(011)_m$ trace



50 nm

